

# What caused the onset of the 1997–1998 El Niño?

Geert Jan van Oldenborgh  
*KNMI, De Bilt, The Netherlands*

April 30, 2022

## Abstract

There has been intense debate about the causes of the 1997–1998 El Niño. One side sees the obvious intense westerly wind events as the main cause for the exceptional heating in summer 1997, the other emphasizes slower oceanic processes. We present a quantitative analysis of all factors contributing to the onset of this El Niño. At six months’ lead time the initial state contributes about 40% of the heating compared with an average year, and the wind about 50%. Compared with 1996, these contributions are 30% and 90% respectively. As westerly wind events are difficult to predict, this limited the predictability of the onset of this El Niño.

## The Problem

The 1997–1998 El Niño was one of the strongest on record. Unfortunately, its onset was not predicted as well as had been hoped (Pearce, 1997). In spite of claims that an El Niño could be predicted a year in advance, most predictions (Stockdale et al., 1998; Ji et al., 1996; Huang and Schneider, 1999; Kleeman et al., 1995) only started to indicate a weak event six months ahead of time. There have therefore been suggestions that El Niño depends not only on internal factors, but also on external noise in the form of weather events in the western Pacific.

The classical picture of El Niño (Bjerknes, 1966; Philander, 1990) is that the usual temperature difference between the warm water near Indonesia and

the ‘cold tongue’ in the eastern equatorial Pacific causes an intensification of the trade winds. These keep the eastern region cool by drawing cold water to the surface. This positive feedback loop is kept in check by nonlinear effects. During an El Niño the loop is broken: a decreased temperature difference causes a slackening or reversal of the trade winds over large parts of the Pacific. This prevents cold water from reaching the surface, keeping the surface waters warm and sustaining the El Niño.

This picture leaves open the question how an El Niño event is triggered and terminated. A variety of mechanisms has been proposed. On long time scales an unstable mode of the nonlinear coupled ocean-atmosphere system may be responsible (Neelin, 1991), either oscillatory or chaotic. Other authors stress the importance of a ‘recharge’ mechanism (Wyrtki, 1975; Jin, 1997), with a built-up of warm water in the western Pacific preceding an El Niño. Another description on shorter time scales is in terms of reflections of equatorial Rossby and Kelvin waves in the thermocline (the interface between warm surface water and the cold water below at about 100 m depth). These would provide the negative feedback that sustains oscillations (Suarez and Schopf, 1988; Battisti and Hirst, 1989; Kessler and McPhaden, 1995). However, short-scale atmospheric ‘noise’ in the form of westerly wind events in the western Pacific may also be essential in triggering an El Niño (Wyrtki, 1985; Kessler et al., 1995).

Here we trace the causes of the onset of last year’s El Niño in May 1997 over the six months from 1 December 1996. This is the time scale over which predictions are currently skillful. Although El Niño is an oscillation of the coupled ocean-atmosphere system, the analysis can be simplified by first studying the response of the ocean to forcing with observed wind stress and heat flux fields. This response contains all time delays. The other part of the loop, the dependence of the wind stress and heat flux on the ocean surface temperature will be discussed separately.

The ocean model used is the Hamburg Ocean Primitive Equation Model, HOPE (Frey et al., 1997; Wolff et al., 1997) version 2.3, which is very similar to the ocean component of the European Centre for Medium-range Weather Forecasts (ECMWF) seasonal prediction system (Stockdale et al., 1998), but restricted to the Pacific Ocean. It is a general circulation model with a horizontal resolution of  $2.8^\circ$ , increased to  $0.5^\circ$  along the equator, and a vertical resolution of 25 m in the upper ocean. It traces the evolution of temperature  $T$ , salinity  $S$ , horizontal velocities  $u, v$  and sea level  $\zeta$ .

This ocean model is forced with daily wind stress  $(\tau_x, \tau_y)$  and heat flux

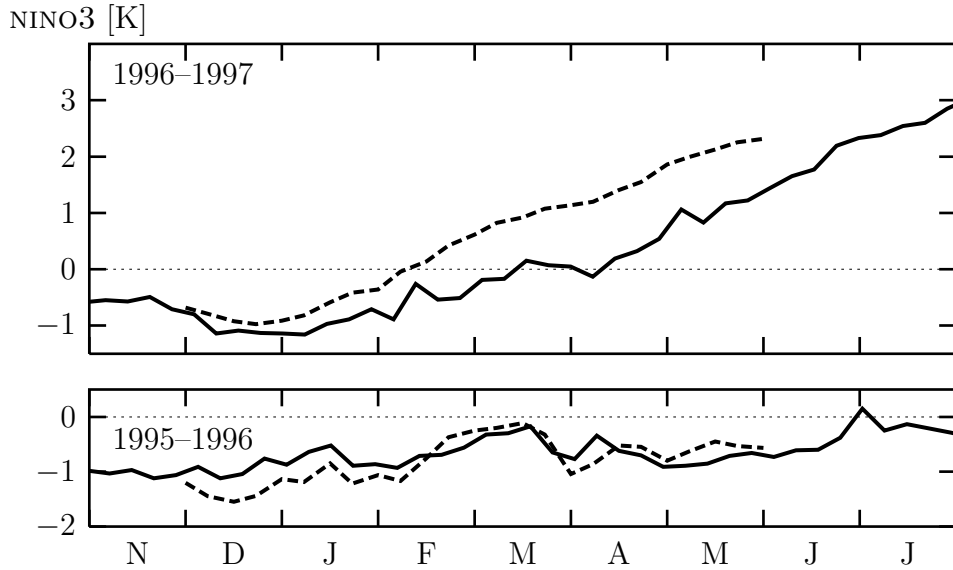


Figure 1: The NINO3 index observed (solid line) and simulated by the six-month forced model runs (dashed lines).

$Q$  from the ECMWF analysis, which in turn uses the excellent system of buoys (McPhaden et al., 1997) that observed this El Niño. Evaporation and precipitation are only implemented as a relaxation to climatological surface salinity. The initial state conditions are ECMWF analysed ocean states. To suppress systematic model errors we subtract a run starting from an average 1 December ocean state forced with average wind and heat fluxes (both 1979–1996 averages (Gibson et al., 1997)).

The model simulates the onset of the 1997–1998 El Niño quite well. We use the NINO3 index  $N_3$ , which is a common measure of the strength of El Niño (the anomalous sea surface temperature in the area 5°S–5°N, 90°W–150°W). In Fig. 1 the weekly observed NINO3 index (Reynolds and Smith, 1994) is shown together with the index in the model run, compared to the same period one year earlier. The model overreacts somewhat to the forcing and simulates a NINO3 index of 2.3 K at 1 June 1997, whereas in reality the index reached this value one month later. In 1995–1996 the simulation follows reality very well.

## The Adjoint Model

The value of the NINO3 index at the end of a model run can be traced back to the model input (initial state, forcing) with an *adjoint model*. The normal ocean model is a (complicated) function  $\mathcal{M}$  that takes as input the state of the ocean at some time  $t_0$  (temperature  $T_0$ , salinity  $S_0$ , etc.). Using the wind stress  $\vec{\tau}_i$  and heat flux  $Q_i$  for each day  $i$  for six months it then produces a final state temperature  $T_n$ . The adjoint model (or backward derivative model) is the related function that takes as input derivatives to a scalar function of the final state, here the NINO3 index,  $\partial N_3 / \partial T_n$ . It goes backward in time and uses the chain rule of differentiation (Giering and Kaminski, 1998) to compute from these (and the forward trajectory) the derivatives  $\partial N_3 / \partial T_0$ ,  $\partial N_3 / \partial S_0$ ,  $\partial N_3 / \partial \vec{\tau}_i$  and  $\partial N_3 / \partial Q_i$ . These derivatives can be interpreted as *sensitivity fields*, giving the effect of a perturbation in the initial state or forcing fields. We can use them to make a Taylor expansion of the NINO3 index to all the input variables:

$$N_3 \approx \frac{\partial N_3}{\partial T_0} \cdot \delta T_0 + \frac{\partial N_3}{\partial S_0} \cdot \delta S_0 + \sum_{\text{days } i} \left( \frac{\partial N_3}{\partial \vec{\tau}_i} \cdot \delta \vec{\tau}_i + \frac{\partial N_3}{\partial Q_i} \cdot \delta Q_i \right) \quad (1)$$

This means that the value of the index is explained as a sum of the influences of initial state temperature and salinity, and the wind and heat forcing during the six months of the run. These influences are each a dot product of the sensitivity to this variable (computed with the adjoint model) multiplied by its deviation from the normal state (extracted from the ECMWF analyses). To minimize higher order terms we take the average derivative from the simulation and the climatology run. We have checked with actual perturbations that the accuracy of the linear approximation Eq. 1 is usually better than about 30% (within the model). Details can be found in van Oldenborgh et al. (1999).

## The 1997–1998 El Niño

For the value of the NINO3 index on 1 June 1997 the linearization Eq. 1 gives a value of 1.8 K, compared with the 2.3 K simulated (and 1.3 K observed), this is within the expected error. The high value is mainly due to the influence

of the westerly wind anomalies (1.0 K) and the initial state temperature on 1 December 1996 (1.1 K). The salinity contributes  $-0.3$  K, with a large uncertainty.

The spatial structure of the influence of the initial state temperature is shown in Fig. 2. The top panel gives the temperature anomaly  $\delta T_0$  along the equator at the beginning of the run (Dec 1996), showing an unusually deep thermocline in the western Pacific and a shallower thermocline in the eastern Pacific. The second frame depicts the sensitivity of the June NINO3 index to temperature anomalies six months earlier,  $\partial N_3 / \partial T_0$ . The third frame is just the product of the previous two; the integral of this over the whole ocean gives the 1.1 K contribution to the NINO3 index mentioned before. The contribution is concentrated in the deeper layer of warm water along the equator in the western Pacific, in agreement with a ‘recharge’ mechanism.

Fig. 3 shows the time structure of the influence of the zonal wind stress. The area under the solid graph gives the total influence, 1.0 K. The main causes of warming are the three peaks in zonal wind stress (dashed line) at the beginning of March, the end of March and the beginning of April, contributing about 0.6 K, 0.3 K and 0.5 K respectively. The peaks correspond with (very) strong westerly wind events in the western Pacific. These generated downwelling Kelvin waves in the thermocline that travelled east and deepened the layer of warm water in the eastern Pacific 2–3 months later, increasing the surface temperature. There was also a strong wind event in December, contributing about 0.4 K over a negative baseline. From Fig. 3 it seems likely that it increased the strength of the later wind events by heating the eastern Pacific in March. The heating effect of the March wind event also gave rise to an increase of the wind stress  $\delta \tau_x$  in May, but this reversal of the trade winds does not yet influence the NINO3 index  $\partial N_3 / \partial \tau_x \cdot \delta \tau_x$ , justifying the uncoupled analysis.

The structure of the peaks in Fig. 3 can be seen more clearly in spatial views. In Fig. 4a the zonal wind stress anomaly  $\delta \tau_x$  is plotted for the second week of March. The westerly wind event corresponds to the large localized westerly anomaly around 150°E. Fig. 4b shows the sensitivity of the NINO3 index in June to the zonal wind stress during this week,  $\partial N_3 / \partial \tau_x$ . This sensitivity consists of two main parts, both equatorially confined. In the western and central Pacific extra westerly wind stress would excite a downwelling Kelvin wave, raising the NINO3 index three months later. In the eastern Pacific the response would be in the form of a Rossby wave. The product of the anomaly and sensitivity fields is shown in Fig. 4c. This gives the influence

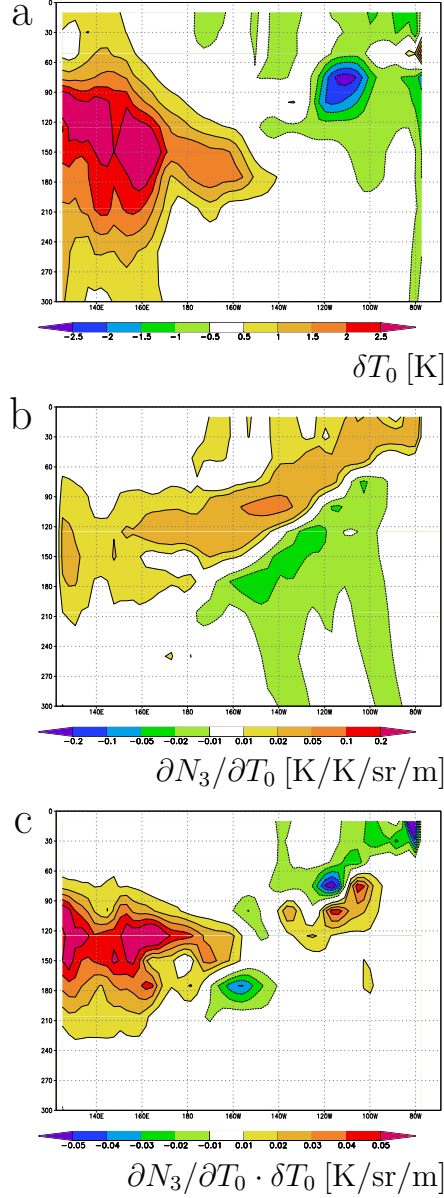


Figure 2: Depth-longitude plots of the effect of the initial state temperature on the NINO3 index in early June. At the top the analyzed temperature anomalies (averaged over  $5^{\circ}\text{S}$ – $5^{\circ}\text{N}$ ) are shown at the beginning of December 1996; the second frame depicts the sensitivity of the ocean to these temperature anomalies and the third the product of these two, which gives the rise in the NINO3 index on June 1 due to the thermal structure six months earlier.

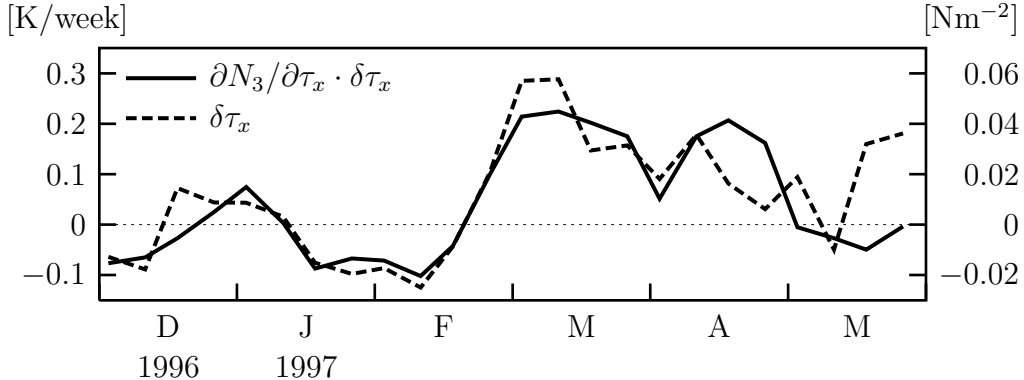


Figure 3: The influence of the zonal wind stress  $\tau_x$  on the NINO3 index at 1 June 1997 during the previous six months (solid line), the average anomalous wind stress over the area  $130^\circ\text{E}$  to  $160^\circ\text{W}$ ,  $5^\circ\text{S}$  to  $5^\circ\text{N}$ .

of zonal wind stress during this week on the NINO3 index, the integral of this field gives the corresponding value (0.22 K) in Fig. 3. The influence is contained in the intersection of the westerly wind event and the equatorial wave guide, and very localized in time and space. The effects of the other wind events are similar.

The question remains whether the big influence of these wind events was due to their strength  $\delta\tau_x$  or to an increased sensitivity of the ocean  $\partial N_3 / \partial \tau_x$ . We therefore repeated the analysis for the same months one year earlier, when the temperature in the eastern Pacific stayed below normal (Fig. 1). The adjoint model gives a NINO3 index of  $-0.6$  K, equal to the simulated index (the observed index was  $-0.7$  K). This index is built up by a large negative influence of the wind stress,  $-1.5$  K, and a positive influence of the heat flux,  $+0.9$  K. The influence of the initial state temperature is also positive, but weaker than in the 1996–1997  $+0.6$  K, and the salinity contributes  $-0.5$  K.

Although the built-up of warm water is also less pronounced, the largest difference is in the influence of the zonal wind stress. The sensitivity to zonal wind stress  $\partial N_3 / \partial \tau_x$  (over the area where its variability is largest) is compared for these two years in Fig. 5. During the time of the strong early March wind event the sensitivity was not very different between the two years, but it was a factor two higher in April 1997 than in April 1996, and lower during the first two months. In all, these differences cannot explain more than a few tenths of a degree difference in the NINO3 index on 1 June.

The difference between an El Niño in 1997 and no El Niño in 1996 can

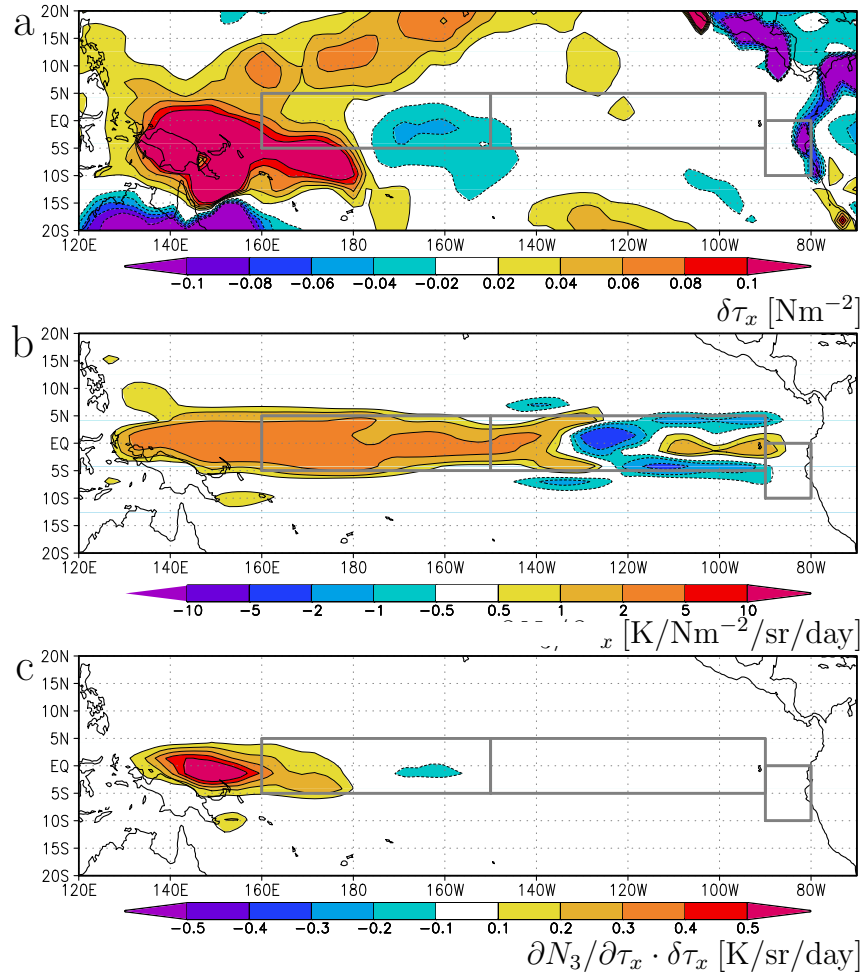


Figure 4: The effect of the March westerly windburst on the NINO3 index in early June. At the top the averaged westerly wind stress anomaly for the week centered on 11 March 1997 is shown, the second frame depicts the sensitivity of the ocean to zonal wind stress and the third the product of these two which gives the rise in the NINO3 index on June 1 due to this wind event.

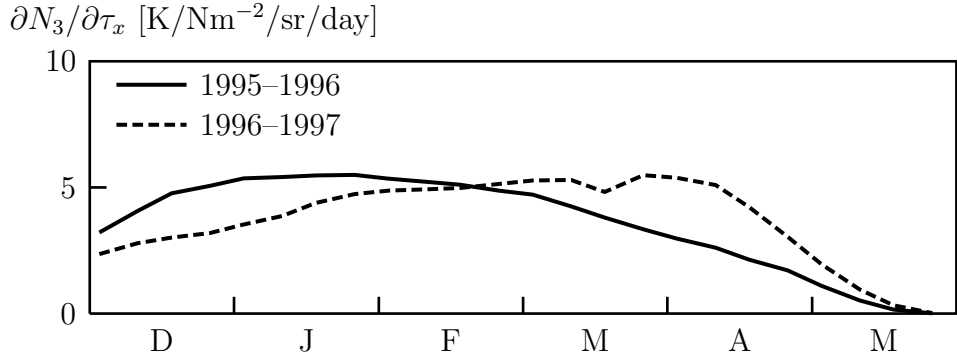


Figure 5: The average sensitivity of the NINO3 index on 1 June to westerly winds in the area defined in Fig. 3.

be attributed for about 30% to an even stronger built-up of warm water in the western Pacific, and for about 90% to the the absence of strong westerly wind events in the western Pacific in the 1995–1996 rain season. A successful prediction scheme will have to predict the intensity of the westerly wind events correctly. However, the year-to-year variability of these wind events does not seem to depend on the state of the Pacific ocean (Slingo et al., 1999), and at the moment is not predictable.

## Conclusions

Using an adjoint ocean model we have shown that a successful prediction of the strong onset of the 1997–1998 El Niño, required a successful prediction of strong westerly wind events in March–April, which in our model contributed about 90% to the strength of the El Niño on 1 June 1997 compared to the situation one year earlier. The sensitivity to these wind events was not significantly different from the year before. The built-up of warm water contributed about 30% of the difference. The strong dependence on the westerly wind events would explain the relatively short lead time for correct predictions of the strong onset of this El Niño.

**Acknowledgments** I would like to thank the ECMWF seasonal prediction group for their help and support and Gerrit Burgers for his part in the construction of the adjoint model. This research was supported by the Nether-

lands Organization for Scientific Research (NWO).

## References

Battisti, D. S. and A. C. Hirst, 1989: Interannual variability in a tropical atmosphere–ocean model: Influence of the basic state, ocean geometry and nonlinearity. *J. Atmos. Sci.*, **46**, 1687–1712.

Bjerknes, J., 1966: A possible response of the atmospheric Hadley circulation to equatorial anomalies of ocean temperature. *Tellus*, **18**, 820–829.

Frey, H., M. Latif, and T. Stockdale, 1997: The coupled GCM ECHO-2. Part I: The tropical Pacific. *Mon. Wea. Rev.*, **125**, 703–720.

Gibson, R., P. Kållberg, S. Uppala, A. Hernandez, A. Nomura, and E. Serrano, 1997: ECMWF re-analysis 1. ERA description. Technical report, ECMWF, Reading, UK.

Giering, R. and T. Kaminski, 1998: Recipes for adjoint code construction. *ACM Trans. Math. Software*, **24**, 437–474.

Huang, B. and E. K. Schneider, 1999: The response of an ocean general circulation model to surface wind stress produced by an atmospheric general circulation model. *Mon. Wea. Rev.*, **in pres**, . Forecasts are published at <http://www.iges.org/ellfb>.

Ji, M., A. Leetmaa, and V. E. Kousky, 1996: Coupled model predictions of ENSO during the 1980s and 1990s at the National Centers for Environmental Prediction. *J. Clim.*, **9**, 3105–3120. Forecasts are under <http://nic.fb4.noaa.gov>.

Jin, F.-F., 1997: An equatorial recharge paradigm for ENSO, part I: Conceptual model. *J. Atmos. Sci.*, **54**, 811–829.

Kessler, W. S. and M. J. McPhaden, 1995: Oceanic equatorial waves and the 1991–93 El Niño. *J. Climate*, **8**, 1757–1774.

Kessler, W. S., M. J. McPhaden, and K. M. Weickman, 1995: Forcing of intraseasonal Kelvin waves in the equatorial Pacific. *J. Geophys. Res.*, **100**, 10613–10631.

Kleeman, R., A. Moore, and N. R. Smith, 1995: Assimilation of subsurface thermal data into a simple ocean model for the initialization of an intermediate tropical coupled ocean–atmosphere forecast model. *Mon. Wea. Rev.*, **123**, 3103–3114. Forecasts are at <http://www.bom.gov.au/bmrc/mrlr/rzk/climfcn3.htm>.

McPhaden, M.J., A.J. Busalacchi, R. Cheney, J.R. Donguy, K.S. Gage, D. Halpern, M. Ji, P. Julian, G. Meyers, G.T. Mitchum, P.P. Niiler, J. Picaut, R.W. Reynolds, N. Smith, and K. Takeuchi, 1997: The Tropical Ocean Global Atmosphere (TOGA) observing system: a decade of progress. *J. Geophys. Res.*, **100**, 14169.

Neelin, J. D., 1991: The slow sea-surface temperature mode and the fast-wave limit: Analytic theory for tropical interannual oscillations and experiments in a hybrid coupled model. *J. Atmos. Sci.*, **48**, 584–606.

Pearce, F., 1997: Sneaky El Niño outwits weather forecasters. *New Scientist*, **31 May**, 6.

Philander, S. G., 1990: *El Niño, La Niña and the Southern Oscillation*. Academic Press, 293 pp.

Reynolds, R. W. and T. M. Smith, 1994: Improved global sea surface analyses using optimum interpolation. *J. Clim.*, **7**, 929–948. NINO indices are available from the Climate Prediction Center at <http://nic.fb4.noaa.gov/data/cddb/altindex.html>.

Slingo, J.M., D. P Rowell, K. R. Sperber, and F. Nortley, 1999: On the predictability of the interannual behaviour of the Madden-Julian Oscillation and its relationship with El Niño. *Quart. J. Roy. Meteorol. Soc.*, **in press**,

Stockdale, T. N., D. L. T. Anderson, J. O. S. Alves, and M. A. Balmaseda, 1998: Global seasonal rainfall forecasts using a coupled ocean–atmosphere model. *Nature*, **392**, 370–373.

Suarez, M. J. and P. S. Schopf, 1988: A delayed action oscillator for ENSO. *J. Atmos. Sci.*, **45**, 3283–3287.

van Oldenborgh, G. J., G. Burgers, S. Venzke, C. Eckert, and R. Giering, 1999: Tracking down the ENSO delayed oscillator with an adjoint OGCM. *Mon. Wea. Rev.*, accepted, . physics/9706007.

Wolff, J.-O., E. Maier-Reimer, and S. Legutke, 1997: The Hamburg Ocean Primitive Equation model HOPE. Technical Report No. 13, Deutsches Klimarechenzentrum, Bundesstr. 55, D-20146 Hamburg, Germany, Hamburg.

Wyrtki, K., 1975: El Niño — the dynamic response of the equatorial Pacific Ocean to atmospheric forcing. *J. Phys. Oceanogr.*, **5**, 572–584.

Wyrtki, K., 1985: Water displacements in the Pacific and the genesis of El Niño. *J. Geophys. Res.*, **90**, 7129–7132.